STUDY ON SEA ICE WITH GMS REAL-TIME DATA *

Li Wanbiao (李万彪), *Zhu Yuanjing* (朱元竞), *Chen Junye* (陈俊晔) and *Zhao Bolin* (赵柏林)

Laboratory for Severe Storm Research, Department of Geophysics, Peking University, Beijing 100871

Received April 21, 1997; revised September 20, 1998

ABSTRACT

By use of GMS-4 infrared brightness temperature and visible albedo data from January to February in 1995, the method for extracting of sea ice parameters is developed. The digital remote sensing picture is obtained on Liaodong Bay. Based on the difference in physical properties between ice and water, a criterion distinguishing ice from water is set up. Ice thickness has been calculated according to the relationship between ice thickness and brightness as well as albedo. Ice concentration is retrieved due to the difference on albedo between ice and water. The results indicate that the accuracy of ice-water distinguishing is 84.8%, the errors of ice thickness and ice concentration are 3.8 cm and 22%, respectively.

Key words: geostationary meteorological satellite (GMS), sea ice, ice-water distinguishing, ice thickness, ice concentration

I. INTRODUCTION

Sea ice is one of the important disasters on the mid and high latitude ocean areas. Great progress has been achieved on the aviation remote sensing (Du et al. 1993) and satellite (NOAA) monitoring (Gong 1993; Huang et al. 1992) of sea ice in China in recent years. Satellite (particular the geostationary satellite) remote sensing is a very effective method to monitor the continuous and wide range sea ice.

Geostationary meteorological satellite (GMS) has several advantages over the polar orbiting satellite for monitoring sea ice. The satellite's altitude (35800 km) tends to minimize the horizontal variations in satellite-observed radiation that are due to atmospheric absorption variations. Also, analyzing sea ice change becomes possible from the continuous satellite observation. Finally, in comparison with NOAA/AVHRR, the probability of obtaining cloud-free views of the ocean surface is largely enhanced at least once per day because of the more observed times. However, GMS-4 contains only two channels (visible: 0.55—0.75 μm; infrared: 10.5—12.5 μm) with relative lower spatial resolutions (visible: 1.75 km, infrared: 7.00 km).

* This work was supported by the National Natural Science Foundation of China (Project No. 49794030).

II. DATA PREPROCESSING

Using the infrared and visible channel data of GMS-4, the study of sea ice has been carried on. These digital real-time image data of GMS-4 were received in January and February 1995, and are processed by the radiation calibration, earth location and albedo solar zenith angle modification. The sea area of Liaodong Bay of China is considered.

The limited measurements of sea ice can be obtained by radar station on the coast and aviation recently. The retrieved sea ice fields by NOAA/AVHRR corrected by these measurements will be used as the contrast fields for verifying the sea ice distributions retrieved by GMS-4.

The retrieved fields (digital distributions of ice thickness and concentration) from NOAA/AVHRR are in the box of 0.1° latitude × 0.1° longitude, the GMS-4 data are matched in the same box. As the GMS-4 data contain about 64 visible pixels or 4 infrared pixels in a box, twice histogram method (Kato 1983) is applied for the extracting of albedo data, and dual-linear interpolation method is adopted for the extracting of infrared brightness temperature data.

The corresponding data of ice-water albedo and brightness temperature are obtained after the data assimilation. Data include 3000 samples, which are derived from the clear GMS-4 data of 20 days at 0332 GMT on Liaodong Bay in January and February of 1995 (1, 3, 6, 7, 12, 14, 15, 16, 18, 24 and 29 in January; 1, 3, 4, 5, 6, 8, 10, 13 and 14 in February). Ice and water samples are 1556 and 1444, respectively.

III. ICE-WATER DISTINGUISHING

The $T-A$ two-dimensional curved surface projection probability charts of ice and water are made separately (T denotes GMS infrared brightness temperature and A visible albedo. The $T-A$ chart is abbreviated hereinafter), and overlap with each other completely (see Fig. 1). Water has high brightness temperature and low albedo, ice has low brightness temperature and high albedo, so ice locates on the down-right of the chart, and water up-left of the chart. Their border is drawn by bend lines ABCD, it can be seen that the water and ice areas are separated largely from each other, but overlap in a small section.

According to the Bayes classification criterion (Ma et al. 1993) of probability principle, ABCD is regarded as the threshold line for the ice-water distinguishing (also see Fig. 1) after the comparison of statistics. The probability of ice-water distinguishing incorrectly is the smallest with the classification. The water area is on the up-left of ABCD, contains 1429 samples including 1208 water samples. The probability of distinguishing incorrectly is 15.3% and that of leaving out is 16.3%. The ice area is on the down-right of ABCD, contains 1571 samples including 1335 ice samples. The probability of distinguishing incorrectly is 15.3% and that of leaving out is 14.2%. Finally the accuracy 84.8% of ice-water distinguishing is obtained.

IV. RETRIEVAL OF ICE THICKNESS

Based on analyzing of all kinds of data of ice thickness, GMS-4 infrared brightness

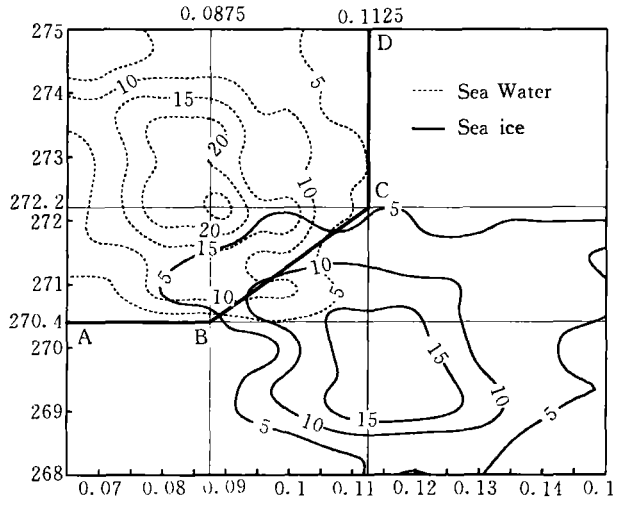

Fig. 1. Distribution of ice-water two-dimensional (albedo and brightness temperature) probability. The figures of contour are sample numbers.

temperature and visible albedo, the ice thickness can be retrieved through the combination of the brightness temperature and albedo, because the higher the albedo is and the lower the brightness temperature is, thus the thicker the ice is.

A corresponding table of ice thickness vs. albedo and brightness temperature is made on the basis of the grid-mesh on $T-A$ surface. The brightness temperature ranges from 268 K to 275 K at intervals of 0.2, while albedo from 0.0625 to 0.15 at intervals of 0.0025. There are 36×36 grid points in total. The corresponding ice thickness in a grid is calculated by the average of all ice thickness data in the same grid. A simple background field is made because the ice samples can not cover the $T-A$ surface completely. In the $T-A$ chart, a line from point (0.0625, 268) to point (0.15, 275) is used as a border. Water is in the up-left of the border and the area of down-right of the border is ice whose thickness is well-distributedly increased from 1 cm in the down-right to 15 cm thickness at the point (0.15, 268). The corresponding table is filled with the background fields, when the ice samples are missing.

A corresponding table made by the data at 0332 GMT in January, is used to retrieve the ice thickness in February of 1995. Figure 2 shows a two-dimensional distribution of ice thickness vs. albedo and brightness temperature based on the corresponding table. The distributions of ice thickness at 0332 GMT in February are retrieved with GMS-4 data. Comparisons of these fields with the contrast fields by NOAA/AVHRR indicate that the mean standard deviation in ice thickness retrieval is 3.8 cm.

V. RETRIEVAL OF ICE CONCENTRATION

The albedo is better than brightness temperature in reflecting the difference of ice and water during the process on seeking the threshold line of ice-water distinguishing on the $T-A$ chart. A best albedo value 0.105 is found when the statistics on albedo around the value 0.1 in the interval of 0.0025 is carried on. With this value as the threshold, the

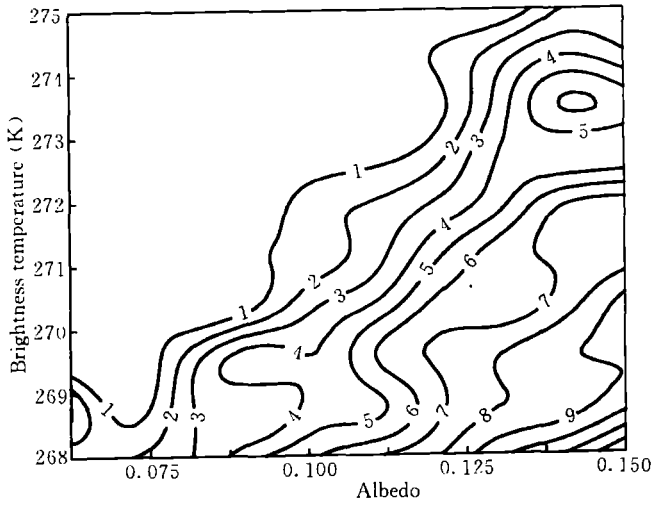

Fig. 2. Two-dimensional (albedo and brightness temperature) distribution of ice thickness. The figures of contour is ice thickness (cm).

accuracy of ice-water distinguishing is 81.8%.

There are about 64 visible pixels of GMS-4 data in a box of 0.1° latitude × 0.1° longitude. The ice pixel numbers can be determined on the basis of the albedo of these pixels. Then ice concentration in the grid box can be obtained by the ratio of the ice pixel numbers to the total pixel numbers of the grid box.

The distribution of ice concentration can be retrieved with GMS-4 data in February 1995 by this method. Comparisons of these fields with the contrast fields by NOAA/AVHRR indicate that the mean correlative coefficient of two fields is 0.74. and the mean standard error in ice concentration retrieval is 22%.

VI. ERROR DISCUSSING

The distributions of ice thickness and concentration are retrieved on the day of 1. 3. 4. 5. 6. 8. 10. 13 and 14 in February of 1995. The GMS-4 retrieval fields at 0332 GMT on January 1 are presented here together with the contrast ice fields by NOAA/AVHRR (Fig. 3 and Fig. 4). The comparisons show that the distributions of sea ice (ice thickness and concentration) retrieved by GMS-4 are in good agreements with the contrast fields by NOAA/AVHRR.

Sea ice situations are monitored by satellite data mainly from NOAA satellite with high spatial resolution and more channels recently. Radar (Kwok et al. 1991) and aviation remote sensing measurements are still the main observing methods. The precisions of sea ice remote sensing, forecasting and being retrieved here by GMS-4 data are listed in Table. 1.

The precision of satellite monitoring can be compared with that of the internal sea ice forecasting because ice can survive for a long time. Table 1 shows that a higher precision of ice retrieved with the GMS-4 dual-channel statistical method, the precision of ice-water distinguishing exceeds the standard of the internal forecasting (Ocean Forecasting

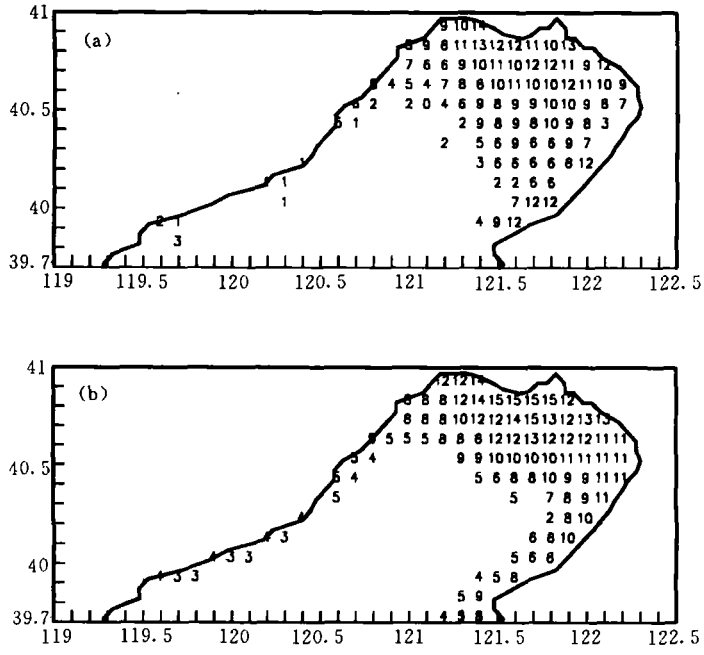

Fig. 3. Comparison between (a) the digital field of sea ice thickness retrieved by GMS-4 at 0332 GMT and (b) the contrast field by NOAA/AVHRR in Liaodong Bay on February 1. 1995. The unit of the thickness is cm.

Observatory of National Ocean Bureau 1986). and ice thickness error is matched with that of the internal and external aviation remote sensing (Du et al. 1993). Moreover. ice concentration is also retrieved. Thus it can be seen that GMS data have a great future for the sea ice monitoring.

Table 1. Comparisons of Sea Ice Measuring Errors

Methods	Ice errors	Accuracy
radar (SAR)		sea-ice classification 63.0%—77.8%
external aviation	error<20 cm. (ice thickness 0—1 m)	
internal aviation	<30%	
internal forecasting		>75% (thickness and range of ice)
GMS-4 dual-channel statistical method	ice thickness standard error is 3.8 cm. concentration 22%	84.8% (ice distinguishing)

There are several sources of possible error in the GMS-4 dual-channel statistical method as follows:

(1) Satellite instrument errors. such as brightness temperature resolution (0.5—

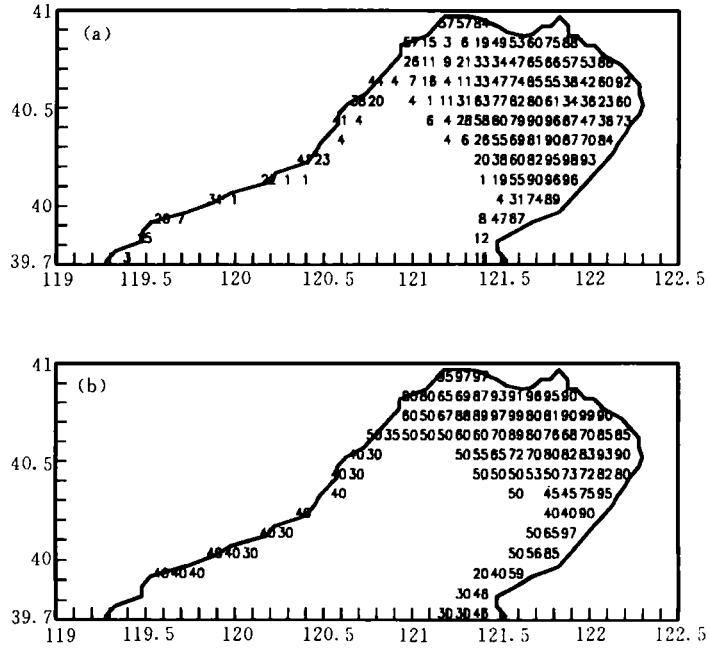

Fig. 4. As in Fig. 3. but for sea ice concentration (the unit of ice concentration is %).

1.5 C):

(2) The error caused by a unified criterion, although the atmospheric conditions are inconsistent;

(3) The frozen temperature of ice is closely related to the ocean salinity. Because of the inconsistent salinity and the different sea surface frozen temperatures in Liaodong Bay, the accuracy for ice distinguishing (also ice range determined) is affected;

(4) Error of contrast field.

VII. CONCLUSION

It is very important for sea ice monitoring theoretically and experimentally. Because of the wider observed area and the better real-time characters of satellite, it is very profitable for ice retrieved by satellite data and then for ice forecasting. Because of the more channels and high space resolution of NOAA satellite, the internal research on ice is mainly focused on the using of the data of NOAA. The ice retrieving from GMS data is still not found. Each of the two satellites has its own good qualities. In this paper we have studied how to use GMS data abundantly and to retrieve the sea ice.

By use of the data of GMS-4 infrared brightness temperature and visible albedo, ice-water distinguishing, ice thickness and concentration retrieving have been carried on. Based upon the comparisons with the sea ice fields retrieved by NOAA/AVHR, it shows that the accuracy of ice-water distinguishing is 84.8%, the errors of ice thickness and ice concentration are 3.8 cm and 22%, respectively. The accuracy is matched with the more advanced standard of the internal and external sea ice monitoring. The dual-channel statistical method here can be applied to the monitoring of ice situations.

REFERENCES

Du Bilan et al. (1993). The technical research of aviation remote sensing ice conditions on the north of Bohai and Huanghai areas. *The National Key Projects on Science and Technology in the Seventh Five Years Periods — A Collection of Research Achievements on Oceanic Environments Numerical Forecasting*. China Ocean Press, Beijing, pp. 240—259 (in Chinese).

Gong Jialong (1993). The method of satellite remote sensing and an operational software package on the real-time monitoring of sea ice and SST in China sea areas. *The National Key Projects on Science and Technology in the Seventh Five Years Periods — A Collection of Research Achievements on Oceanic Environments Numerical Forecasting*. China Ocean Press, Beijing, pp. 199—211 (in Chinese).

Huang Runheng et al. (1992). Extracting of sea ice parameters from the NOAA satellite image data. *Advances in Remote Sensing in China*. Wan-guo Academic Press, Hongkong, pp. 306 — 311 (in Chinese).

Kato, Y. (1983). Extracting of meteorological elements from images data of geostationary meteorological satellite. *Meteorological Research Note*, **148**: 1—57 (in Japanese).

Kwok, R. et al. (1991). Application of neural networks to sea ice classification using polarimetric SAR images. *Remote Sensing: Global Monitoring for Earth Management*, I: 85—88.

Ma Kaiyu et al. (1993). *The Principles and Methods of Climatic Statistics*. China Meteor. Press, Beijing, pp. 208—218 (in Chinese).

Ocean Forecasting Observatory of National Ocean Bureau (1986). A brief description in broadcasting of ocean forecasting. *Ocean Forecasting*, **2**: 73—76 (in Chinese).